

Hepatic, intestinal, renal and plasma hydrolysis of prodrugs in human, cynomolgus monkey, dog and rat - implications for in vitro-in vivo extrapolation of clearance of prodrugs

Haruka Nishimuta, J. Brian Houston and Aleksandra Galetin

Centre for Applied Pharmacokinetic Research, Manchester Pharmacy School, University of Manchester, Manchester, United Kingdom (H.N., J.B.H., A.G.); Pharmacokinetics Research Laboratory, Dainippon Sumitomo Pharma Co., Ltd., Osaka, Japan (H.N.)

Running title: Species and system differences in hydrolysis activities

Corresponding author: Dr Aleksandra Galetin

Centre for Applied Pharmacokinetic Research,
Manchester Pharmacy School,
The University of Manchester, Stopford Building
Oxford Road,
Manchester, M13 9PT, UK
Tel: (+) 44 161 275 6886
Fax: (+) 44 161 275 8349
Email: Aleksandra.Galetin@manchester.ac.uk

Pages: 34
Tables: 5
Figures: 3
References: 44
Abstract: 263
Introduction: 765
Discussion: 1504

Abbreviations: CES, carboxylesterase; CL_{int} , intrinsic clearance; $CL_{int,h}$ hepatic intrinsic clearance; $CL_{int,hepatocytes}$, intrinsic hydrolysis clearance obtained in hepatocytes; $CL_{int,LS9}$, intrinsic hydrolysis clearance obtained in liver S9; $CL_{int,IS9}$ intrinsic hydrolysis clearance obtained in intestinal S9; CMBL, carboxymethylenebutenolidase; IS9, intestinal S9; KS9, kidney S9; LS9, liver S9; LC-MS/MS, high-performance liquid chromatography - tandem mass spectrometry; PMSF, phenylmethylsulfonyl fluoride; PON, paraoxonase; $t_{1/2}$, half-life

Abstract

Hydrolysis plays an important role in metabolic activation of prodrugs. In the current study, species and in vitro system differences in hepatic and extrahepatic hydrolysis were investigated for 11 prodrugs. Ten prodrugs in the dataset are predominantly hydrolyzed by carboxylesterases (CES), whereas olmesartan medoxomil is also metabolized by carboxymethylenebutenolidase (CMBL) and paraoxonase. Metabolic stabilities were assessed in cryopreserved hepatocytes, liver S9 (LS9), intestinal S9 (IS9), kidney S9 (KS9) and plasma from human, monkey, dog and rat. Of all the preclinical species investigated, monkey hydrolysis $CL_{int,hepatocytes}$ were the most comparable to human hepatocyte data. Perindopril and candesartan cilexetil showed the lowest and highest $CL_{int,hepatocytes}$, respectively regardless of the species investigated. Scaled hydrolysis $CL_{int,LS9}$ were generally higher than $CL_{int,hepatocytes}$ in all species investigated, with the exception of dog. In the case of human and dog intestinal S9, hydrolysis CL_{int} could not be obtained for CES1 substrates, whereas hydrolysis for CES2 and CMBL substrates was detected in IS9 and KS9 from all species. Pronounced species differences were observed in plasma; hydrolysis of CES substrates was only evident in rat. Predictability of human $CL_{int,h}$ was assessed for 8 CES1 substrates using hepatocytes and LS9; extrahepatic hydrolysis was not considered due to high stability of these prodrugs in intestinal and kidney S9. On average, predicted oral $CL_{int,h}$ from hepatocyte data represented 20% of the observed value; the under-prediction was pronounced for high clearance prodrugs, consistent with predictability of P450/conjugation clearance from this system. Prediction bias was less apparent with LS9, in particular for high clearance prodrugs, highlighting the application of this in vitro system for investigation of prodrugs.

Introduction

The prodrug concept has been increasingly used over recent years; 20% of all small molecules approved in the period of 2000-2008 were prodrugs (Stella, 2010; Huttunen et al., 2011; Dahan et al., 2012). Many prodrugs are inactive compounds with either carboxyl-ester, thio-ester or amide (Taketani et al., 2007; Laizure et al., 2013) which are subsequently hydrolyzed to an active drug; the extent of hydrolysis markedly affects the pharmacological activity and/or toxicity of these compounds. The intentional esterification to a prodrug has been used across different classes of drugs (e.g., antivirals, ACE inhibitors), mostly to improve drug absorption and bioavailability (Imai, 2006; Li et al., 2008). This concept has recently been taken further in a form of carrier-mediated prodrug to target peptide transporter 1 in the small intestine (Gupta et al., 2013).

Carboxylesterases (CES), in particular CES1 and CES2, represent major enzymes involved in the hydrolysis of structurally diverse prodrugs (Sato and Hosokawa, 1998; Imai, 2006; Hosokawa, 2008). Human CES1 tends to hydrolyze esters with a large acyl moiety relative to the alcohol group (e.g., benazepril), opposite to CES2 substrates with a generally small acyl group, as in the case of candesartan cilexetil (Supplemental Figure 1) (Taketani et al., 2007; Laizure et al., 2013). Recent studies have highlighted the role of carboxymethylenebutenolidase (CMBL) for the hydrolysis of prodrugs in the liver and intestine (e.g., olmesartan medoxomil) (Ishizuka et al., 2010). CMBL is a relatively novel hydrolysis enzyme and any potential overlap in its substrates with CES is not well characterized. Cellular localization of these enzymes differs, as CES are present both in the membrane and cytosol (Sato and Hosokawa, 1998; Fujiyama et al., 2010), whereas CMBL is a predominantly cytosolic enzyme (Ishizuka et al., 2013), emphasizing careful choice of *in vitro* system for adequate characterization of hydrolysis. In addition, paraoxonase 1 (PON1), predominantly

located in plasma (Bahar et al., 2012), hydrolyzes lactones and aromatic carboxylic acid esters (Fukami and Yokoi, 2012; Ishizuka et al., 2012).

CES1 expression based on mRNA data is the highest in the liver both in human and preclinical species (Supplemental Table 1), suggesting its key role in hydrolysis of prodrugs (Williams et al., 2010). However, human CES1 is also expressed in the lung, heart and kidney, but to a lesser extent (Satoh et al., 2002). This dominant CES1 expression relative to CES2 in the liver was also confirmed by proteomic data, with an average protein expression level of 402 and 30 pmol/mg protein reported in human liver microsomes for CES1 and CES2, respectively (Sato et al., 2012). In addition to small intestine, human CES2 mRNA data have also been reported for kidney and to minor extent colon and heart (Satoh et al., 2002; Quinney et al., 2005). Analogous to human, CES2 mRNA has been quantified in liver and/or intestine of preclinical species, although data in some species/other tissues are sparse (Supplemental Table 1). Expression data highlight the need for consideration of extrahepatic hydrolysis, analogous to role of these organs in P450 and conjugation metabolism (Galetin and Houston, 2006; Paine et al., 2006; Cubitt et al., 2009; Gertz et al., 2010; Nishimuta et al., 2011; Gill et al., 2012). In addition, significant species differences were observed in CES expression in plasma, with high levels reported for rat, but not human, monkey and dog plasma (Li et al., 2005; Berry et al., 2009). CMBL is highly expressed in liver, intestine and kidney across different species except in the dog intestine (Ishizuka et al., 2013).

Although studies have reported some species differences in CES mediated hydrolysis of prodrugs (Prueksaritanont et al., 1996; Yoshigae et al., 1998; Williams et al., 2011), general paucity of data on the activity of CES and/or other hydrolytic enzymes in different systems across species is evident. Therefore, the aim of the present study was to investigate species and in vitro system differences in hydrolysis of 11 selected prodrugs. Most of the prodrugs in the

dataset are predominantly metabolized by CES1 (8/11), whereas candesartan cilexetil and mycophenolate mofetil are substrates for both CES1 and CES2 (Laizure et al., 2013). In addition, olmesartan medoxomil is hydrolyzed by CMBL and PON1, with a minor CES contribution. Intrinsic clearance (CL_{int}) values were obtained in cryopreserved hepatocytes, liver S9 (LS9), intestinal S9 (IS9) and kidney S9 (KS9); same in vitro systems were used in human, cynomolgus monkey, beagle dog and Sprague-Dawley rat. The importance of intestinal and renal hydrolysis relative to hepatic was assessed. Finally, the predictability of in vitro CL_{int} hydrolysis data generated in human hepatocytes and LS9 was investigated for a subset of 8 CES1 prodrugs using reported in vivo clearance following oral administration.

Materials and Methods

Chemicals. Benazepril hydrochloride was purchased from Wako Pure Chemical Industries Ltd (Osaka, Japan); candesartan cilexetil, perindopril erbumine, quinapril hydrochloride and ramipril were purchased from LKT Laboratories (St. Paul, MN); cilazapril, trandolapril, temocapril hydrochloride, mycophenolate mofetil and olmesartan medoxomil were purchased from Toronto Research Chemicals (North York, ON, Canada); oseltamivir phosphate was purchased from Selleck Chemicals (Houston, TX). All other reagents and solvents were of analytical grade and were commercially available.

Subcellular fractions. Liver S9 from Sprague-Dawley rat (pool of 400 male), beagle dog (pool of 12 male), cynomolgus monkey (pool of 13 male) and human (pool of 50) were purchased from Xenotech, LLC (Lenexa, KS, USA). Kidney S9 from Sprague-Dawley rat (pool of 149 male), beagle dog (pool of 5 male), cynomolgus monkey (pool of 5 male) and human (pool of 4) were purchased from the same supplier. Intestinal S9 from Sprague-Dawley rat (pool of 40 male), beagle dog (individual, male), cynomolgus monkey (individual, male) and human (individual, male) were purchased from the same supplier. To avoid any potential enzyme stability issues, no freeze-thaw cycles were applied during the experiments. Only intestinal S9 prepared in the absence of phenylmethylsulfonyl fluoride (PMSF) were used considering reported inhibitory effect of PMSF on CES activity in the process of isolation of enterocytes via elution method (Kleingeist et al., 1998; Morgan et al., 2008).

Hepatocytes. Cryopreserved hepatocytes from Sprague-Dawley rat (pool of 8 male), beagle dog (pool of 3 male), cynomolgus monkey (pool of 3 male) and human (pool of 20, equal number of male and female) were purchased from Xenotech, LLC (Lenexa, KS, USA).

Plasma. Pooled plasma fraction treated by heparin sodium salt from Sprague-Dawley rat, beagle dog and cynomolgus monkey were purchased from Valley Biomedical Products and

Services, Inc. (Winchester, VA, USA). Pooled plasma fraction treated by heparin sodium salt from human was purchased from Kohjin Bio Co., Ltd. (Saitama, Japan).

Metabolic stabilities in liver, intestinal and kidney S9. Compounds investigated (200 nM) were incubated at 37°C in 100 μ L of 50 mM phosphate buffer (pH 7.4). The same conditions were used for liver, intestinal and kidney S9 from Sprague-Dawley rat, beagle dog, cynomolgus monkey and human. In the case of kidney, we conducted preliminary studies only for substrates of CES2 and CMBL, which are highly expressed in human kidney, namely; candesartan cilexetil, mycophenolate mofetil and olmesartan medoxomil. Linearity of metabolic activities for S9 concentration (0.01–1 mg S9 protein/mL) and incubation time (5 min, 15 min or 60 min) were confirmed and the optimal reaction conditions were established for each compound. The final concentration of acetonitrile in the incubation mixture was 0.5% (v/v). After preincubation at 37°C for 5 min, the reactions were initiated by the addition of the substrates and stopped by addition of 200 μ L of ice-cold acetonitrile. Control samples were incubated using the same method as in the absence of substrates; substrates were added after addition of ice-cold acetonitrile. The reaction mixtures were spiked with 200 μ L of acetonitrile containing the internal standard, 200 nM flecainide. The mixtures were centrifuged at 3400g for 10 min to remove precipitated protein. The supernatants were then filtrated using 0.45- μ m 96-well filter plates (Varian Inc., Palo Alto, CA, USA). The filtrate was diluted 2-fold using distilled water and transferred to 96-well plates, and a 10- μ L portion was then injected onto a high-performance liquid chromatography/tandem mass spectrometry (LC-MS/MS) system.

Preparation of hepatocytes. The vials of cryopreserved hepatocytes were thawed by immersion for 1.5 min in a 37°C water bath. After thawing, the hepatocyte suspension was poured into Tube A of the hepatocyte isolation kit (XenoTech LLC) containing supplemented Dulbecco's modified Eagle's medium and isotonic Percoll and then centrifuged (70 g) for 5 min

at 25°C. After the supernatant was removed, the cells were resuspended in 5 ml of supplemented Dulbecco's modified Eagle's medium in Tube B of the hepatocyte isolation kit. The number of viable cells was then determined using trypan blue staining and confirmed the viability was >80%. Subsequently, the cells were resuspended in the remaining medium from Tube B and then centrifuged (50 g) for 3 min at 25°C, followed by removal of the supernatant. Finally, the cells were re-suspended in the Krebs-Henseleit buffer at a density of $0.1\text{--}2.0 \times 10^6$ viable cells/ml for the stability experiment.

Metabolic stabilities in hepatocytes. The hepatocyte suspension (150 μL) was distributed in 24-wells plates and incubated in CO_2 incubator under 5% CO_2 at 37°C for 10 min. The reaction was initiated by adding an equal volume (150 μL) of Krebs-Henseleit buffer containing drugs (the final concentration is 200 nM in acetonitrile) to the hepatocyte suspension. The buffer containing drugs were prewarmed at 37°C for 10 min before the stability studies. The final concentration of acetonitrile was 0.05% (v/v) in the incubation mixture. After incubation at 37°C for 0, 5, 15, 60 and 120 min, 50 μL of the incubation mixture was added into 200 μL of acetonitrile containing the internal standard, 200 nM flecainide. The mixtures were centrifuged at 3400g for 10 min to remove precipitated protein. The supernatants were then filtrated using 0.45- μm 96-well filter plates (Varian Inc., Palo Alto, CA, USA). The filtrate was diluted 2-fold using distilled water and transferred to 96-well plates, and a 10 μL portion was then injected onto LC-MS/MS.

Metabolic stabilities in plasma. Compounds investigated were incubated at 37°C in 100 μL of plasma from Sprague-Dawley rat, beagle dog, cynomolgus monkey or human at a final concentration of 200 nM. Linearity of metabolic activities for incubation time (10 s, 30 s, 1 min, 2 min, 5 min, 15 min or 60 min) was confirmed in the preliminary studies and the optimal reaction conditions were established for each compound. The final concentration of acetonitrile

in the incubation mixture was 0.5% (v/v). After preincubation at 37°C for 5 min, the reactions were initiated by the addition of the substrates and stopped by addition of 200 μ L of ice-cold acetonitrile. Control samples were incubated using the same method as in the absence of substrates; substrates were added after addition of ice-cold acetonitrile. The reaction mixtures were spiked with 200 μ L of acetonitrile containing the internal standard, 200 nM flecainide. The mixtures were centrifuged at 3400g for 10 min to remove precipitated protein. The supernatants were then filtrated using 0.45- μ m 96-well filter plates (Varian Inc., Palo Alto, CA, USA). The filtrate was diluted 2-fold using distilled water and transferred to 96-well plates, and a 10 μ L portion was then injected onto LC-MS/MS.

The fraction unbound in human plasma (f_{u_p}) for 8 CES1 substrates was determined using a high-throughput dialysis method. The method was considered adequate due to high stability of these prodrugs in the human plasma samples. Dialysis membranes with a 10 kDa molecular mass cut-off were purchased from Harvard Apparatus (Holliston, MA). Compounds (1 μ M, final) with human plasma were added to the acceptor chambers whereas phosphate buffered saline was added to the donor chamber. The dialysis plate was placed in an incubator at 37 °C for 22h on a plate rotator. After equilibrium had been reached, 10 μ L of samples in the acceptor chamber were mixed with 40 μ L of phosphate buffered saline and 40 μ L of samples in the donor chamber were mixed with 10 μ L of human plasma. These samples were then mixed with 200 μ L of methanol containing the internal standard (200 nM flecainide) and centrifuged at 4500 rpm for 10 min to remove precipitated protein. The supernatants were filtered using 0.45 μ m 96-well filter plates (Varian, Inc., Palo Alto, CA) and analysed using LC-MS/MS.

LC-MS/MS. Concentrations of compounds in samples were measured using an LC-MS/MS system consisting of an API4000 mass spectrometer (Applied Biosystems, Forester City, CA, USA) with a Shimadzu 20A series HPLC system. Chromatography was performed using an

Inertsil ODS-3 column (3- μ m particle size, 2.1 \times 50 mm, GL Science, Tokyo, Japan) warmed to 40°C. The mobile phase consisted of 0.1% formic acid (A) and acetonitril (B). The flow rate was 0.2 mL/min, and the gradient conditions for elution were as follows: gradient [min, B%] = [0, 10]-[1, 90]-[4, 90]-[4.1, 10]-[7, 10]. Mass spectrometric conditions for individual analytes are given in Table 1.

Data Analysis. The peak area ratios of test compounds to internal standard were used for the calculation in all experiments. The mean value of triplicate determinations was plotted versus the incubation time on a semi-logarithmic scale, and the slope was determined by linear-regression analysis as depletion rate constant (k (min^{-1})). For liver S9, intestinal S9 and hepatocytes, the CL_{int} values were calculated using the following equations:

$$\text{CL}_{\text{int}} \text{ (mL/min/mg protein)} = \frac{V \cdot k}{\text{protein}_{\text{S9}}} \cdot \frac{1}{f_{\text{u, S9}}} \quad (1)$$

$$\text{CL}_{\text{int}} \text{ (mL/min/10}^6 \text{ cells)} = \frac{V \cdot k}{\text{number}_{\text{hepatocytes}}} \cdot \frac{1}{f_{\text{u, hepatocytes}}} \quad (2)$$

Where V is the initial incubation volume (mL), $\text{protein}_{\text{S9}}$ is the initial amount of S9 protein in incubation (mg), $\text{number}_{\text{hepatocytes}}$ is the initial number of hepatocytes in incubation ($\times 10^6$ cells), $f_{\text{u, S9}}$ is fraction unbound in S9 incubation, $f_{\text{u, hepatocytes}}$ is fraction unbound in hepatocytes incubation. The $f_{\text{u, S9}}$ and $f_{\text{u, hepatocytes}}$ values were predicted as reported previously (Hallifax and Houston, 2006; Kilford et al., 2008) assuming that binding in S9 was comparable to that in human liver microsomes at the same protein concentrations. Predictive tools were applied to avoid any potential stability issues over prolonged periods in buffer during the equilibrium dialysis experiments. Protein concentration used in the in vitro experiments was low (whenever possible) to minimize any potential issues associated with nonspecific binding. Most of the prodrugs investigated showed predicted $f_{\text{u, S9}}$ or $f_{\text{u, hepatocytes}}$ of >0.8 at the protein/cell

concentration used and the subsequent nonspecific binding correction was not implemented. The only exception were candesartan cilexetil (logP = 6.1) (Detroja et al., 2011) and mycophenolate mofetil (logP = 3.0).

In vitro CL_{int} obtained in hepatocytes (mL/min/ 10^6 cells) were scaled by Equation 3 to give an in vivo CL_{int} (mL/min/g liver) using hepatocellularity values of 120×10^6 cells/g liver for human, monkey and rat, and 240×10^6 cells/g liver for dog (Houston and Galetin, 2008; Hosea et al., 2009):

$$CL_{int, \text{hepatocytes}} \text{ (mL/min/g liver)} = CL_{int} \text{ (mL/min/} 10^6 \text{ cells)} \cdot \frac{\text{hepatocytes}}{\text{liver weight}} \quad (3)$$

To allow direct comparison of the intestinal and hepatic S9 data, CL_{int} values (mL/min/mg S9 protein) were scaled to the CL_{int} values to per g tissue using Equation 4 and 5 for human LS9 and IS9, respectively. S9 scaling factors for preclinical species were assumed to be the same as the values reported for human (Houston and Galetin, 2008; Cubitt et al., 2011).

$$CL_{int, \text{LS9}} \text{ (mL/min/g liver)} = CL_{int} \text{ (mL/min/mg S9 protein)} \cdot 121 \text{ (mg S9 protein/g liver)} \quad (4)$$

$$CL_{int, \text{IS9}} \text{ (mL/min/g intestine)} = CL_{int} \text{ (mL/min/mg S9 protein)} \cdot 38.6 \text{ (mg S9 protein/g intestine)} \quad (5)$$

Due to lack of kidney S9 scaling factor, we used the two approaches – using the same scaling factor as for liver S9 (121 mg S9 protein/g; (Houston and Galetin, 2008)) (A) or combining specific kidney microsomal scaling factor (12.8 mg S9 protein/g; (Gill et al., 2012)) with a liver cytosolic scaling factor (80.7 mg S9 protein/g; (Houston and Galetin, 2008)) resulting in a value of 93.5 mg S9 protein/g (Scaling factor B).

When CL_{int} values could not be estimated due to high stability (>90% of the compound still remaining after 60 min (S9) or 120 min incubation (hepatocytes)), a nominal value of 0.1 mL/min/g liver was assigned for these drugs in Figures 1 and 2; these compounds were not included in the subsequent analysis shown in Figures 3 and 4. Discrepancy in animal hydrolysis CL_{int} data relative to human were assessed by geometric fold error (gmfe). This analysis was only performed for hepatocytes due to high stability of a number of compounds in liver S9 or intestinal S9 from preclinical species.

In vitro-in vivo extrapolation of human prodrug clearance. Due to lack of i.v. clearance data reported for prodrugs, predictability of human hydrolysis CL_{int} data was assessed against oral clearances. $CL_{int,h}$ values after oral drug administration were estimated using Equation 6 for a subset of 8 CES1 substrates (Pang and Rowland, 1977; Gertz et al., 2010)

$$CL_{int,h} \text{ (mL/min/kg)} = \frac{D}{AUC \cdot fu_p/R_b} \cdot F_G \cdot F_a \quad (6)$$

where D/AUC represents the hepatic blood clearance obtained from mean plasma data after correcting for renal excretion (where applicable) and blood to plasma distribution ratio (R_b). Renal excretion was minimal for most of the prodrugs (<1%) with the exception of quinapril, perindopril and oseltamivir (3-14%, Supplementary Material, Table 4). The fu_p represents the fraction unbound in plasma, D represents the oral drug dose (mg/kg), AUC represents the area under the drug concentration-time curve (mg/min/mL), F_G is intestinal availability and F_a is the fraction absorbed. Oral clearance data for 8 CES1 substrates and R_b for oseltamivir were collated from the literature (Supplementary Material, Table 4). The R_b value for 7 remaining prodrugs was assumed to be as 0.55, assumption used previously for acidic drugs (Kilford et al.,

2009). The F_G values for all 8 prodrugs were assumed to be 1, considering their high stability in intestinal S9 (see Results). In addition, absorption of these drugs was assumed to be complete ($F_a = 1$) due to their high solubility (>1 mg/mL in buffer and FaSSIF for all 8 prodrugs, in house data) and low dose number (<0.3 for all the prodrugs in the dataset). The lowest PAMPA permeability in this dataset was obtained for perindopril, which translated to effective permeability of 1.34×10^{-4} cm/s, confirming the validity of $F_a = 1$ assumption (Lennernas, 2014). The unbound $CL_{int,h}$ from human hepatocytes or liver S9 (Equations 3 and 4, respectively) were scaled using average liver weight of 21.4 g of liver/kg.

Results

CL_{int} values were obtained for 11 prodrugs in four different species across a range of in vitro systems, namely cryopreserved hepatocytes, LS9, IS9 and KS9 using substrate depletion approach. The CL_{int} values were corrected for nonspecific binding and scaled to CL_{int} per g of tissue to allow comparison among different tissues and/or species. In addition, stability of prodrugs in plasma samples from each species was investigated. Predictability of human hydrolysis CL_{int} data was assessed for a subset of 8 prodrugs with reported in vivo data.

Assessment of hydrolysis activity in hepatocytes across species. Individual CL_{int} values ($\text{mL}/\text{min}/10^6$ cells) obtained for 11 prodrugs in human, monkey, dog and rat hepatocytes are listed in Table 2. The correlation between CL_{int} ($\text{mL}/\text{min}/\text{g}$ liver) scaled from human and animal hepatocytes data for all the compounds investigated is shown in Figure 1.

The human $CL_{int,hepatocytes}$ ranged three orders of magnitude from 0.73–740 $\text{mL}/\text{min}/\text{g}$ liver for perindopril and candesartan cilexetil, respectively. Similarly, the monkey $CL_{int,hepatocytes}$ ranged from 0.30–930 $\text{mL}/\text{min}/\text{g}$ liver for perindopril and candesartan cilexetil, respectively (Figure 1A). The monkey CL_{int} values for seven drugs were within 3-fold of the human CL_{int} values, with an excellent agreement in the CL_{int} values in the case of candesartan cilexetil, mycophenolate mofetil and temocapril. The monkey $CL_{int,hepatocytes}$ showed a 2.7-fold deviation from human hydrolysis CL_{int} data obtained in the same cellular system. The most pronounced outlier was oseltamivir where the monkey $CL_{int,hepatocytes}$ value represented only 6% of the corresponding value in human hepatocytes.

Analogous to monkey and human, dog $CL_{int,hepatocytes}$ showed a wide range (1.4–3400 $\text{mL}/\text{min}/\text{g}$ liver) with perindopril and candesartan cilexetil being the drugs with lowest and highest CL_{int} values (Figure 1B). The dog hydrolysis CL_{int} were within 3-fold of the human hepatocyte values values for seven compounds; however, increased divergence from human

$CL_{int,hepatocyte}$ data was apparent (gmfe of 3.6). The largest disagreement between dog and human hepatocyte data was seen for mycophenolate mofetil and oseltamivir. Mycophenolate mofetil dog $CL_{int,hepatocytes}$ was 29-fold higher than the human CL_{int} value, whereas oseltamivir was highly stable in dog hepatocytes ($CL_{int} < 0.1$ mL/min/g liver) relative to human cells (11 mL/min/g liver, Table 2).

Of all the preclinical species investigated, rat hydrolysis $CL_{int,hepatocytes}$ showed the most pronounced disagreement with human data (gmfe=4.4, Figure 1C). In general, most of the CL_{int} values obtained in rat hepatocytes were higher than human data obtained in the same in vitro system; the difference was up to 52-fold in the case of temocapril (Supplementary Material, Figure 2). Analogous to the trends seen in monkey and dog $CL_{int,hepatocytes}$ data, oseltamivir was the outlier, with the rat CL_{int} value representing <10% of the human CL_{int} .

Assessment of hydrolysis activity in LS9 across species. Individual CL_{int} values (mL/min/mg S9 protein) obtained in human, monkey, dog and rat liver S9 are shown in Table 3. A three orders of magnitude range in human $CL_{int,LS9}$ was observed (0.48–650 mL/min/g liver); perindopril and candesartan cilexetil were extremes, as seen in hepatocyte CL_{int} data (Figure 2). Analogous to hepatocytes, oseltamivir CL_{int} data in monkey LS9 were 6-fold lower than in human. In contrast, monkey $CL_{int,LS9}$ were higher than human for candesartan cilexetil, mycophenolate mofetil, olmesartan medoxomil and temocapril (up to 23-fold). In general, the rat $CL_{int,LS9}$ values for CES1 substrates were higher than the human values, whereas opposite trend was seen for dog $CL_{int,LS9}$ data relative to human (candesartan cilexetil exception). Differences in $CL_{int,LS9}$ values across three preclinical species were not pronounced for candesartan cilexetil, mycophenolate mofetil and perindopril (up to 5-fold), in contrast to trandolapril, quinapril and ramipril where >100-fold difference in scaled $CL_{int,LS9}$ was observed (Figure 2A).

Comparison of $CL_{int,hepatocytes}$ and $CL_{int,LS9}$. On average, $CL_{int,LS9}$ were higher than $CL_{int,hepatocytes}$ values in all species other than dog. Human $CL_{int,LS9}$ data for trandolapril, perindopril, oseltamivir and candesartan cilexetil were in excellent agreement with $CL_{int,hepatocytes}$, whereas the $CL_{int,LS9}$ for all the remaining prodrugs was higher than in human hepatocytes (up to 20-fold in the case of mycophenolate mofetil) (Figure 3A).

In contrast to human LS9, a number of compounds showed high stability in animal LS9 and CL_{int} could not be obtained (Figure 3B-D). In particular, this was evident for perindopril, oseltamivir and quinapril where CL_{int} data were not determined in two out of three preclinical species investigated (Table 3). Analogous to human, mycophenolate mofetil monkey CL_{int} data showed the most pronounced system differences (50-fold higher value obtained in monkey LS9 compared with hepatocytes). This trend was consistent across all preclinical species, as the $CL_{int,LS9}$ values for this prodrug were higher than the $CL_{int,hepatocytes}$. The number of stable prodrugs in dog LS9 was the largest among species investigated and CL_{int} was not determined for 4/11 prodrugs (Figure 3C). The range of scaled dog $CL_{int,LS9}$ for the remaining drugs was 0.38–2900 mL/min/g liver; as in previous cases candesartan cilexetil showed the highest CL_{int} .

Assessment of hydrolysis activity in intestinal S9 across species. CL_{int} values (mL/min/mg S9 protein) obtained in human, monkey, dog and rat intestinal S9 fractions are listed in Table 4. In the case of human intestine, the CL_{int} for CES1 substrates (drugs 1-8 in each Table) was not detected ($CL_{int,IS9} < 0.002$ mL/min/mg S9 protein). In contrast, the $CL_{int,IS9}$ values for CES2 and CMBL substrates, ranged from 0.4 to 2.9 mL/min/mg S9 protein for olmesartan medoxomil and candesartan cilexetil, respectively. Unlike in human, the CL_{int} were detected for CES1 substrates in monkey and rat IS9. However, intestinal hydrolysis clearance values in both of these preclinical species were generally low for these drugs ($CL_{int} < 0.1$ mL/min/mg S9 protein for all the drugs investigated, with the exception of temocapril). The

monkey $CL_{int,IS9}$ values for CES2 and CMBL substrates were either comparable (candesartan cilexetil and olmesartan medoxomil) or up to 17-fold higher than human IS9 CL_{int} (mycophenolate mofetil). Analogous to human, dog $CL_{int,IS9}$ for eight CES1 substrates were not detected in dog intestine (Table 4). For the remaining CES2 and CMBL substrates, trends were inconsistent with either human or monkey IS9 data; this discrepancy was in particular evident in the case of mycophenolate mofetil where CL_{int} was <0.1% of the human IS9 estimate. The rat $CL_{int,IS9}$ values for CES2 and CMBL substrates were on average 30% of the human $CL_{int,IS9}$ (Table 4).

Assessment of intestinal hydrolysis relative to hepatic. The comparison of CL_{int} values obtained in LS9 relative to IS9 in each individual species is shown in Figure 2B. It is evident that the hepatic hydrolysis CL_{int} were higher than intestinal regardless of the species investigated. The dataset was reduced in human and dog S9 data, due to high stability of CES1 substrates in corresponding IS9. The ratio of monkey $CL_{int,LS9}/CL_{int,IS9}$ for CES1 substrates ranged from 0.8–6 for perindopril and cilazapril, respectively. Across all species, difference in hepatic hydrolysis CES1 CL_{int} values relative to intestine was the most pronounced in rat, with on average 92-fold higher CL_{int} in LS9 (37 to 131-fold for temocapril and ramipril, respectively).

For CES2 and CMBL substrates, the ratio of human $CL_{int,LS9}/CL_{int,IS9}$ ranged from 4-13 for olmesartan medoxomil and candesartan cilexetil, respectively. Data in preclinical species reflected this trend of higher CL_{int} values in liver hydrolysis relative to intestine. However, species differences were evident, as illustrated nicely in the case of mycophenolate mofetil. Intestinal and hepatic hydrolysis were comparable in cyno (within 2-fold), in contrast to >2000 $CL_{int,LS9}/CL_{int,IS9}$ ratio seen in dog, illustrating very different contribution of intestinal hydrolysis to the first pass effect and bioavailability of this prodrug across preclinical species.

Assessment of hydrolysis activity in kidney S9. CL_{int} values (mL/min/mg S9 protein) in KS9 of each species were only obtained for candesartan cilexetil, mycophenolate mofetil and olmesartan medoxomil (Table 5); hydrolysis was detected in KS9 from all species investigated. For candesartan cilexetil and mycophenolate mofetil, the $CL_{int,KS9}$ (mL/min/mg S9 protein) values in preclinical species were higher than those in human (on average 5.4 to 33-fold respectively), with the most pronounced differences seen in dog $CL_{int,KS9}$ data relative to human. In the case of olmesartan medoxomil, the $CL_{int,KS9}$ (mL/min/mg S9 protein) among all four species were within 7-fold. The scaled $CL_{int,KS9}$ (mL/min/g kidney) was calculated using two alternative kidney S9 scaling factor; details are shown in Supplemental Table 3. Human scaled $CL_{int,KS9}$ (mL/min/g kidney) values for candesartan cilexetil and mycophenolate mofetil (CES2 substrates) were lower than the $CL_{int,IS9}$ (mL/min/g intestine), in contrast to olmesartan medoxomil where they were comparable.

Assessment of hydrolysis activity in plasma. CES substrates showed high stability in human, monkey and dog plasma as >90% of the drug remained after 60min incubation. The only exception was rat plasma, where the hydrolysis was evident, even in the case of CES substrates, with the half-life ($t_{1/2}$) values ranging from 0.11-5.2 min for trandolapril and oseltamivir, respectively (Supplemental Table 2). In contrast, olmesartan medoxomil hydrolysis was seen in plasma from both human and preclinical species ($t_{1/2}$ <0.1 min, in contrast to $t_{1/2}$ of 2.3 min in rat plasma).

In vitro-in vivo extrapolation of hydrolysis clearance for CES1 prodrugs. The ability of in vitro CL_{int} hydrolysis data obtained in human hepatocytes and LS9 to predict oral clearance for 8 CES1 substrates was investigated; no i.v. clearance data were available for any of the prodrugs investigated. Hepatic hydrolysis was assumed to be the only contributor to the oral clearance considering high stability of these prodrugs in intestinal S9. In vitro-in vivo

extrapolation was limited to human, due to limited availability of data in preclinical species; in this case oral clearances were not considered due to intestinal hydrolysis observed in some preclinical species.

Hepatocyte data predicted $CL_{int,h}$ for 4/8 prodrugs within 3-fold of the observed data. However, under-prediction trend was particularly evident for high clearance prodrugs ($CL_{int,h} > 550$ ml/min/kg), as the predicted clearance represented only 2-14% of the observed value for quinapril and benazepril, respectively. This trend was not as apparent when LS9 data were used, as temocapril and benazepril clearances were predicted relatively well (up to 50% of observed); in contrast, prediction of trandolapril and quinapril clearance was comparable to hepatocytes (4 and 11% of the observed, respectively). Prediction bias was less apparent with LS9 (gmfe of 3.2 vs. 5 seen in the case of hepatocytes), highlighting the utility of this subcellular fraction for the prediction of human hydrolysis clearance.

Discussion

The current study represents the most comprehensive analysis to date of the species and in vitro system differences (hepatocytes vs. S9) in hydrolysis CL_{int} generated under standardized conditions. In addition, the importance of extrahepatic hydrolysis (intestine and kidney) relative to hepatic has been assessed. Quantitative prediction of in vivo hydrolysis clearance focused on human data only; inconsistent or unavailable in vivo data in preclinical species limited our attempts to assess species differences in the predictability of hydrolysis clearance.

Species differences in hepatic hydrolysis activity. The hydrolysis CL_{int} could be obtained in hepatocytes for all the drugs investigated in both human and preclinical species. Regardless of the species, perindopril and candesartan cilexetil were the prodrugs with the lowest and highest CL_{int} , whereas the rank order of other compounds varied.

Across all species investigated, the monkey hepatocyte data showed the most comparable hydrolysis CL_{int} relative to human hepatocytes (evident in particular for candesartan cilexetil, mycophenolate mofetil and temocapril, Figure 1A), in agreement with previous studies in recombinant CES (Williams et al., 2011) and high homology of amino acid sequence reported between cyno and human CES1 and CES2 (Taketani et al., 2007; Hosokawa, 2008; Imai and Ohura, 2010). The most pronounced differences in hydrolysis $CL_{int,hepatocytes}$ in preclinical species relative to human were seen in rat (Figure 1C); esterase family in this preclinical species includes multiple enzymes with 67–77% homology with human CES1 (Taketani et al., 2007; Hosokawa, 2008). Dog hepatocytes data showed a comparable wide range in hydrolysis CL_{int} to other species and good agreement with human $CL_{int,hepatocyte}$ data for a number of low and high clearance prodrugs (e.g., temocapril and candesartan cilexetil); however, discrepancy to human data ($gmfe=3.6$) was more pronounced compared to monkey $CL_{int,hepatocytes}$. Oseltamivir was

generally more stable in all animal hepatocytes relative to human; this trend was particularly evident in dog, as >90% of the drug was stable after 120 min. Dog CES1 shows lower homology with human CES1 (80%) compared with monkey (Taketani et al., 2007; Hosokawa, 2008) which may rationalize some species difference in substrate recognition, especially considering structure similarities of CES1 substrates investigated (with the exception of oseltamivir, Supplemental Figure 1). The homology of amino acid sequence between human and dog CES2 is currently unknown.

Comparison of $CL_{int,LS9}$ and $CL_{int,hepatocytes}$ across species. In the current analysis of 11 prodrugs, the scaled $CL_{int,hepatocytes}$ values were generally lower than the $CL_{int,LS9}$ values in all species, with the exception of dog (Figures 2 and 3). In human, the fold range in $CL_{int,LS9}$ was analogous to hepatocytes, highlighting the utility of LS9 for the characterization of prodrugs in human. However, it is important to note that some of the low clearance compounds in animal hepatocytes (e.g., perindopril, oseltamivir and quinapril) were more metabolically stable in animal LS9 (under the conditions selected) and therefore CL_{int} data could not be determined in all the preclinical species investigated. This stability could not be associated with any methodological differences, as all LS9 fractions were obtained from the same supplier.

Subsequently, in vitro-in vivo extrapolation of hydrolysis CL_{int} data was performed using data obtained in human hepatocytes and LS9. A subset of 8 CES1 substrates with available clearance data following prodrug oral administration was selected, as plasma concentrations of prodrugs after intravenous dosing are often very low and/or not reported, with most data available for the active metabolite. The dataset covered a 75-fold range in observed $CL_{int,h}$, with perindopril and temocapril on the lower and higher end, respectively. Use of hydrolysis hepatocytes data resulted in reasonably good prediction of low clearance prodrugs (50% within 3-fold). However, overall under-prediction trend was evident (5-fold bias), in agreement with

trends reported previously for P450 substrates (Hallifax et al., 2010). This trend was particularly apparent for high clearance prodrugs, as the predicted clearance was <15% of the observed value. For certain prodrugs in this range (e.g., trandolapril), the extent of under-prediction was comparable between hepatocytes and LS9 (predicted CL_{int} was approximately 4% of the in vivo value regardless of the system). However, this under-prediction trend was not evident for all high clearance prodrugs when LS9 data were used, emphasizing promising application of this subcellular in vitro system for the prediction of human hydrolysis clearance. Unfortunately, predictability of in vitro hydrolysis CL_{int} from individual preclinical species was not possible; this kind of analysis would increase the confidence for the subsequent predictive use of human hydrolytic data obtained in the same cellular system/subcellular fraction.

Species differences in intestinal and kidney hydrolysis activity. The metabolic activities for CES1 substrates were not detected in human intestine, in contrast to CES2 and CMBL substrates (Figure 2B and Table 4); the findings were generally in agreement with expression data reported for these enzymes in human intestine (Hosokawa, 2008; Ishizuka et al., 2013). The scaled human $CL_{int,IS9}$ values were lower than the $CL_{int,LS9}$ values for CES2 and CMBL substrates (Figure 2B), suggesting lower expression levels per g tissue of these hydrolases in intestine. Analogous to human, CES1 substrates were also metabolically stable in dog intestinal S9 data, whereas opposite trends were seen in the case of monkey and rat IS9 (Table 4). Surprisingly, the metabolic activities for two CES2 substrates were detected in dog IS9; although the $CL_{int,IS9}$ value for mycophenolate mofetil was low, in particular relative to dog liver S9 data, candesartan cilexetil $CL_{int,IS9}$ was the highest across all species (Table 4). This result was in contrast to reported lack of expression of both CES1 and CES2 in dog intestine (Hosokawa, 2008), indicating potential contribution of additional hydrolysases. The latter is most likely the reason for observed hydrolysis of CES1 substrate temocapril in rat IS9 (Table 4),

opposite to CES expression reported in this species. In the case of olmesartan medoxomil, the lowest CL_{int} obtained in dog IS9 supported minimal CMBL expression levels reported in dog intestine relative to other species (Ishizuka et al., 2013). There was no consistency in differences seen in animal intestinal hydrolysis CL_{int} for CES2 and CMBL substrates relative to human IS9. In addition, differences in the contribution of intestinal hydrolysis to the first pass effect and bioavailability were evident across preclinical species relative to human (e.g., mycophenolate mofetil).

An important consideration is that human, monkey and dog intestinal S9 were prepared from a single individual which may bias the analysis; however, pooled samples prepared without the use of PMSF (CES inhibitor) during the isolation process were not available. In addition, due to lack of data, the intestinal and liver S9 scaling factors for preclinical species were assumed to be the same as human. However, a number of issues have already been highlighted (Cubitt et al., 2011) with respect to the value of human intestinal cytosolic scaling factor (obtained from limited number of samples prepared by mucosal scraping method, no information on the variability) which also propagate here for the scaling of hydrolysis data. In addition, single intestinal S9 scaling factor was used and no potential regional differences were accounted for, which all may impact the analysis of the relevance of intestinal hydrolysis relative to hepatic. Similar problems occurred in the case of kidney data, where general lack of cytosolic/S9 scaling factors led to the use of indirect values (liver), emphasizing the need for more work in this area. In particular if the data were to be used in physiologically-based models to simulate concentration-time profiles of prodrugs and their active metabolites in relevant tissues of interest (safety concern or to assess potential drug-drug interaction risk). Hydrolysis activities were detected in kidney S9 for CES2 and CMBL substrates only (Table 5), in agreement with

expression data reported for these enzymes in the kidney across species (Supplemental Table 1).

Assessment of metabolic stability of prodrugs in plasma highlighted very clear species differences, with fast hydrolysis observed for CES substrates only in rat plasma. For olmesartan medoxomil, PON1 substrate, the metabolic activity in human plasma was comparable to monkey and dog and in all cases significantly more pronounced than in rat, emphasizing the need for consideration of these species differences when performing *in vivo* studies in preclinical species.

In summary, the systematic analysis of species and system differences was performed for 11 prodrugs. Hydrolysis CL_{int} data obtained in monkey hepatocytes were the most comparable to human for the current dataset. The importance of intestinal hydrolysis and species difference in its potential contribution to the overall bioavailability has been illustrated for CES2 and CMBL substrates. Uncertainty in scaling factors, in particular highlighted in the case of kidney and intestinal S9 data, may impact the analysis of the relevance of extrahepatic hydrolysis relative to hepatic. For the first time, the predictive utility of hydrolysis CL_{int} obtained in human hepatocytes and liver S9 was assessed. Reduced prediction bias observed with liver S9 data, in particular for high clearance prodrugs, highlights the application of this subcellular fraction for the characterization of hydrolysis clearance and its prediction. Further evaluation of this *in vitro* system using the extended dataset of prodrugs is needed.

Authorship Contributions

Participated in research design: Nishimuta, Galetin

Conducted experiments: Nishimuta

Performed data analysis: Nishimuta, Galetin

Wrote or contributed to the writing of the manuscript: Nishimuta, Houston, Galetin

References

- Bahar FG, Ohura K, Ogihara T and Imai T (2012) Species difference of esterase expression and hydrolase activity in plasma. *J Pharm Sci* **101**:3979-3988.
- Berry LM, Wollenberg L and Zhao Z (2009) Esterase activities in the blood, liver and intestine of several preclinical species and humans. *Drug Metab Lett* **3**:70-77.
- Cubitt HE, Houston JB and Galetin A (2009) Relative importance of intestinal and hepatic glucuronidation-impact on the prediction of drug clearance. *Pharm Res* **26**:1073-1083.
- Cubitt HE, Houston JB and Galetin A (2011) Prediction of human drug clearance by multiple metabolic pathways: integration of hepatic and intestinal microsomal and cytosolic data. *Drug Metab Dispos* **39**:864-873.
- Dahan A, Khamis M, Agbaria R and Karaman R (2012) Targeted prodrugs in oral drug delivery: the modern molecular biopharmaceutical approach. *Expert Opin Drug Deliv* **9**:1001-1013.
- Detroja C, Chavhan S and Sawant K (2011) Enhanced antihypertensive activity of candesartan cilexetil nanosuspension: formulation, characterization and pharmacodynamic study. *Sci Pharm* **79**:635-651.
- Fujiyama N, Miura M, Kato S, Sone T, Isobe M and Satoh S (2010) Involvement of carboxylesterase 1 and 2 in the hydrolysis of mycophenolate mofetil. *Drug Metab Dispos* **38**:2210-2217.
- Fukami T and Yokoi T (2012) The emerging role of human esterases. *Drug Metab Pharmacokinet* **27**:466-477.
- Galetin A and Houston JB (2006) Intestinal and hepatic metabolic activity of five cytochrome P450 enzymes: impact on prediction of first-pass metabolism. *J Pharmacol Exp Ther* **318**:1220-1229.
- Gertz M, Harrison A, Houston JB and Galetin A (2010) Prediction of human intestinal first-pass metabolism of 25 CYP3A substrates from in vitro clearance and permeability data. *Drug Metab Dispos* **38**:1147-1158.
- Gill KL, Houston JB and Galetin A (2012) Characterization of in vitro glucuronidation clearance of a range of drugs in human kidney microsomes: comparison with liver and intestinal glucuronidation and impact of albumin. *Drug Metab Dispos* **40**:825-835.
- Gupta D, Varghese Gupta S, Dahan A, Tsume Y, Hilfinger J, Lee KD and Amidon GL (2013) Increasing oral absorption of polar neuraminidase inhibitors: a prodrug transporter approach applied to oseltamivir analogue. *Mol Pharm* **10**:512-522.
- Hallifax D, Foster JA and Houston JB (2010) Prediction of human metabolic clearance from in vitro systems: retrospective analysis and prospective view. *Pharm Res* **27**:2150-2161.

- Hallifax D and Houston JB (2006) Binding of drugs to hepatic microsomes: comment and assessment of current prediction methodology with recommendation for improvement. *Drug Metab Dispos* **34**:724-726.
- Hosea NA, Collard WT, Cole S, Maurer TS, Fang RX, Jones H, Kakar SM, Nakai Y, Smith BJ, Webster R and Beaumont K (2009) Prediction of human pharmacokinetics from preclinical information: comparative accuracy of quantitative prediction approaches. *J Clin Pharmacol* **49**:513-533.
- Hosokawa M (2008) Structure and catalytic properties of carboxylesterase isozymes involved in metabolic activation of prodrugs. *Molecules* **13**:412-431.
- Houston JB and Galetin A (2008) Methods for predicting in vivo pharmacokinetics using data from in vitro assays. *Curr Drug Metab*. **9**:940-951.
- Huttunen KM, Raunio H and Rautio J (2011) Prodrugs--from serendipity to rational design. *Pharmacol Rev* **63**:750-771.
- Imai T (2006) Human carboxylesterase isozymes: catalytic properties and rational drug design. *Drug Metab Pharmacokinet* **21**:173-185.
- Imai T and Ohura K (2010) The role of intestinal carboxylesterase in the oral absorption of prodrugs. *Curr Drug Metab* **11**:793-805.
- Ishizuka T, Fujimori I, Kato M, Noji-Sakikawa C, Saito M, Yoshigae Y, Kubota K, Kurihara A, Izumi T, Ikeda T and Okazaki O (2010) Human carboxymethylenebutenolidase as a bioactivating hydrolase of olmesartan medoxomil in liver and intestine. *J Biol Chem* **285**:11892-11902.
- Ishizuka T, Fujimori I, Nishida A, Sakurai H, Yoshigae Y, Nakahara K, Kurihara A, Ikeda T and Izumi T (2012) Paraoxonase 1 as a major bioactivating hydrolase for olmesartan medoxomil in human blood circulation: molecular identification and contribution to plasma metabolism. *Drug Metab Dispos* **40**:374-380.
- Ishizuka T, Yoshigae Y, Murayama N and Izumi T (2013) Different hydrolases involved in bioactivation of prodrug-type angiotensin receptor blockers: carboxymethylenebutenolidase and carboxylesterase 1. *Drug Metab Dispos* **41**:1888-1895.
- Kilford PJ, Gertz M, Houston JB and Galetin A (2008) Hepatocellular binding of drugs: correction for unbound fraction in hepatocyte incubations using microsomal binding or drug lipophilicity data. *Drug Metab Dispos* **36**:1194-1197.
- Kilford PJ, Stringer R, Sohal B, Houston JB and Galetin A (2009) Prediction of drug clearance by glucuronidation from in vitro data: use of combined cytochrome P450 and UDP-glucuronosyltransferase cofactors in alamethicin-activated human liver microsomes. *Drug Metab Dispos* **37**:82-89.

- Kleingeist B, Bocker R, Geisslinger G and Brugger R (1998) Isolation and pharmacological characterization of microsomal human liver flumazenil carboxylesterase. *J Pharm Pharm Sci* **1**:38-46.
- Laizure SC, Herring V, Hu Z, Witbrodt K and Parker RB (2013) The role of human carboxylesterases in drug metabolism: have we overlooked their importance? *Pharmacotherapy* **33**:210-222.
- Lennernas H (2014) Human in vivo regional intestinal permeability: importance for pharmaceutical drug development. *Mol Pharm* **11**:12-23.
- Li B, Sedlacek M, Manoharan I, Boopathy R, Duysen EG, Masson P and Lockridge O (2005) Butyrylcholinesterase, paraoxonase, and albumin esterase, but not carboxylesterase, are present in human plasma. *Biochem Pharmacol* **70**:1673-1684.
- Li F, Maag H and Alfredson T (2008) Prodrugs of nucleoside analogues for improved oral absorption and tissue targeting. *J Pharm Sci* **97**:1109-1134.
- Morgan ET, Goralski KB, Piquette-Miller M, Renton KW, Robertson GR, Chaluvadi MR, Charles KA, Clarke SJ, Kacevska M, Liddle C, Richardson TA, Sharma R and Sinal CJ (2008) Regulation of drug-metabolizing enzymes and transporters in infection, inflammation, and cancer. *Drug Metab Dispos* **36**:205-216.
- Nishimuta H, Sato K, Yabuki M and Komuro S (2011) Prediction of the intestinal first-pass metabolism of CYP3A and UGT substrates in humans from in vitro data. *Drug Metab Pharmacokinet* **26**:592-601.
- Paine MF, Hart HL, Ludington SS, Haining RL, Rettie AE and Zeldin DC (2006) The human intestinal cytochrome P450 "pie". *Drug Metab Dispos* **34**:880-886.
- Pang KS and Rowland M (1977) Hepatic clearance of drugs. I. Theoretical considerations of a "well-stirred" model and a "parallel tube" model. Influence of hepatic blood flow, plasma and blood cell binding, and the hepatocellular enzymatic activity on hepatic drug clearance. *J Pharmacokinet Biopharm* **5**:625-653.
- Prueksaritanont T, Gorham LM, Hochman JH, Tran LO and Vyas KP (1996) Comparative studies of drug-metabolizing enzymes in dog, monkey, and human small intestines, and in Caco-2 cells. *Drug Metab Dispos* **24**:634-642.
- Quinney SK, Sanghani SP, Davis WI, Hurley TD, Sun Z, Murry DJ and Bosron WF (2005) Hydrolysis of capecitabine to 5'-deoxy-5-fluorocytidine by human carboxylesterases and inhibition by loperamide. *J Pharmacol Exp Ther* **313**:1011-1016.
- Sato Y, Miyashita A, Iwatsubo T and Usui T (2012) Simultaneous absolute protein quantification of carboxylesterases 1 and 2 in human liver tissue fractions using liquid chromatography-tandem mass spectrometry. *Drug Metab Dispos* **40**:1389-1396.

- Satoh T and Hosokawa M (1998) The mammalian carboxylesterases: from molecules to functions. *Annu Rev Pharmacol Toxicol* **38**:257-288.
- Satoh T, Taylor P, Bosron WF, Sanghani SP, Hosokawa M and La Du BN (2002) Current progress on esterases: from molecular structure to function. *Drug Metab Dispos* **30**:488-493.
- Stella VJ (2010) Prodrugs: Some thoughts and current issues. *J Pharm Sci* **99**:4755-4765.
- Taketani M, Shii M, Ohura K, Ninomiya S and Imai T (2007) Carboxylesterase in the liver and small intestine of experimental animals and human. *Life Sci* **81**:924-932.
- Williams ET, Bacon JA, Bender DM, Lowinger JJ, Guo WK, Ehsani ME, Wang X, Wang H, Qian YW, Ruterbories KJ, Wrighton SA and Perkins EJ (2011) Characterization of the expression and activity of carboxylesterases 1 and 2 from the beagle dog, cynomolgus monkey, and human. *Drug Metab Dispos* **39**:2305-2313.
- Williams ET, Wang H, Wrighton SA, Qian YW and Perkins EJ (2010) Genomic analysis of the carboxylesterases: identification and classification of novel forms. *Mol Phylogenet Evol* **57**:23-34.
- Yoshigae Y, Imai T, Horita A, Matsukane H and Otagiri M (1998) Species differences in stereoselective hydrolase activity in intestinal mucosa. *Pharm Res* **15**:626-631.

Figure Legends

Figure 1. Correlation of the CL_{int} values in hepatocytes between human and monkey (A), dog (B) or rat (C).

The numbers allocated per compound are as listed in Tables. Scaling to CL_{int} (mL/min/g liver) was done using Equation 3. For highly stable compounds ($CL_{int} < 0.001$ mL/min/ 10^6 cells after 120 min), nominal value of 0.1 mL/min/g liver was used. The solid and dashed lines represent line of unity and a 3-fold range, respectively.

Figure 2. Comparison of scaled animal and human hydrolysis CL_{int} values obtained in LS9 (A). Comparison between the $CL_{int,LS9}$ values and $CL_{int,LS9}/CL_{int,LS9}$ values for human, monkey, dog and rat (B).

The numbers allocated per compound are as listed in Tables. Scaling to CL_{int} (mL/min/g liver or mL/min/g intestine) was done using Equation 4 and 5. For highly stable compounds ($CL_{int} < 0.002$ mL/min/mg S9 protein after 60 min), the CL_{int} values could not be obtained and were not considered in this Figure.

Figure 3. Comparison of the CL_{int} values between in liver S9 and hepatocytes for human (A), monkey (B), dog (C) and rat (D).

The numbers allocated per compound are as listed in Tables. Scaling to CL_{int} (mL/min/g liver) was done using Equations 3 and 4. When >90% of the compound still remained after either 60 min (S9) or 120 min (hepatocytes), the CL_{int} values could not be obtained and were plotted as nominal value of 0.1 mL/min/g liver. The solid and dashed lines represent line of unity and a 3-fold range, respectively.

Figure 4. In vitro-in vivo extrapolation of human hydrolysis CL_{int} data for obtained in either human hepatocytes or liver S9. Observed $CL_{int,h}$ were estimated from plasma clearance data following oral administration of prodrugs, assuming negligible contribution of intestinal hydrolysis and complete absorption.

Table 1. Mass spectrometric conditions for compounds investigated and internal standard with details on mass transitions.

No.	Compounds	Internal Standard	Electrospray Ionization	<i>m/z</i>	Collision Energy (eV)
1	Benazepril	Flecainide	Negative	423.1 > 173.9	-28
2	Cilazapril	Flecainide	Negative	416.1 > 166.9	-28
3	Quinapril	Flecainide	Negative	437.1 > 187.9	-30
4	Trandolapril	Flecainide	Positive	431.2 > 234.3	29
5	Perindopril	Flecainide	Positive	369.2 > 172.3	27
6	Ramipril	Flecainide	Negative	415.1 > 166	-34
7	Temocapril	Flecainide	Positive	477.2 > 190.2	45
8	Oseltamivir	Flecainide	Positive	313.2 > 165.8	27
9	Candesartan cilexetil	Flecainide	Negative	609.1 > 99	-68
10	Mycophenolate mofetil	Flecainide	Negative	432.2 > 244.8	-44
11	Olmesartan medoxomil	Flecainide	Negative	557.1 > 149	-62
	Flecainide	N.A.	Positive	415.1 > 398	33
		N.A.	Negative	413.2 > 269.9	-28

N.A., not applicable.

Table 2. CL_{int} values obtained in hepatocytes of human, monkey, dog and rat

No.	Compounds	CL _{int,hepatocytes} (mL/min/10 ⁶ cells)			
		human	monkey	dog	rat
1	Benazepril	0.031 ± 0.0096	0.0066 ± 0.0026	0.0094 ± 0.0022	0.085 ± 0.032
2	Cilazapril	0.044 ± 0.0017	0.019 ± 0.0037	0.0065 ± 0.00077	0.15 ± 0.0062
3	Quinapril	0.0061 ± 0.0010	0.0036 ± 0.0012	0.0066 ± 0.00052	0.12 ± 0.012
4	Trandolapril	0.022 ± 0.0027	0.0043 ± 0.00025	0.013 ± 0.0040	0.041 ± 0.0025
5	Perindopril	0.0060 ± 0.0012	0.0025 ± 0.00038	0.0060 ± 0.0057	0.0046 ± 0.00080
6	Ramipril	0.025 ± 0.0014	0.0038 ± 0.00083	0.010 ± 0.00055	0.053 ± 0.017
7	Temocapril	0.063 ± 0.0066	0.076 ± 0.011	0.028 ± 0.0058	3.3 ± 1.2
8	Oseltamivir	0.089 ± 0.019	0.0062 ± 0.0032	– ^a	0.0059 ± 0.0030
9	Candesartan cilexetil	6.2 ± 1.1	7.7 ± 0.64	14 ± 0.42	7.0 ± 0.54
10	Mycophenolate mofetil	0.16 ± 0.11	0.16 ± 0.11	2.3 ± 0.26	0.30 ± 0.043
11	Olmesartan medoxomil	0.12 ± 0.037	0.24 ± 0.10	0.072 ± 0.023	0.81 ± 0.10

Each value presents the mean ± S.D. (n=3)

^a CL_{int} values could not be obtained. The remaining ratio of the compounds incubated for 120 min was >90%

Table 3. CL_{int} values in liver S9 of human, monkey, dog and rat

No.	Compounds	CL _{int,LS9} (mL/min/mg S9 protein)			
		human	monkey	dog	rat
1	Benazepril	0.11 ± 0.0078	0.020 ± 0.0072	– ^a	0.16 ± 0.017
2	Cilazapril	0.17 ± 0.0090	0.15 ± 0.059	0.024 ± 0.014	0.79 ± 0.057
3	Quinapril	0.028 ± 0.016	– ^a	– ^a	0.17 ± 0.0068
4	Trandolapril	0.021 ± 0.0015	– ^a	0.0031 ± 0.0012	0.10 ± 0.0023
5	Perindopril	0.0040 ± 0.00031	0.0018 ± 0.00031	– ^a	– ^a
6	Ramipril	0.061 ± 0.0083	– ^a	0.0055 ± 0.0015	0.25 ± 0.0048
7	Temocapril	0.22 ± 0.045	5.0 ± 2.5	0.074 ± 0.018	4.0 ± 1.8
8	Oseltamivir	0.067 ± 0.0065	0.011 ± 0.00074	– ^a	– ^a
9	Candesartan cilexetil	5.4 ± 0.80	16 ± 1.8	24 ± 9.0	12 ± 3.9
10	Mycophenolate mofetil	3.4 ± 0.41	10 ± 0.27	5.2 ± 0.66	2.0 ± 0.066
11	Olmesartan medoxomil	0.47 ± 0.057	5.4 ± 0.47	0.72 ± 0.021	0.62 ± 0.075

Each value presents the mean ± S.D. (n=3)

^a CL_{int} values could not be obtained. The remaining ratio of the compounds incubated for 60 min was >90%

(CL_{int} < 0.002 mL/min/mg S9 protein).

Table 4. CL_{int} values in intestinal S9 of human, monkey, dog and rat

No.	Compounds	CL _{int,S9} (mL/min/mg S9 protein)			
		human	monkey	dog	rat
1	Benazepril	– ^a	0.019 ± 0.0063	– ^a	0.0069 ± 0.00068
2	Cilazapril	– ^a	0.073 ± 0.014	– ^a	0.025 ± 0.0056
3	Quinapril	– ^a	0.0074 ± 0.0027	– ^a	0.0041 ± 0.00084
4	Trandolapril	– ^a	– ^a	– ^a	0.0037 ± 0.00021
5	Perindopril	– ^a	0.0072 ± 0.0016	– ^a	– ^a
6	Ramipril	– ^a	0.0035 ± 0.0013	– ^a	0.0060 ± 0.00037
7	Temocapril	– ^a	15 ± 2.5	– ^a	0.34 ± 0.12
8	Oseltamivir	– ^a	– ^a	– ^a	– ^a
9	Candesartan cilexetil	2.9 ± 0.69	3.3 ± 1.1	8.0 ± 1.9	0.77 ± 0.46
10	Mycophenolate mofetil	0.83 ± 0.096	14 ± 3.0	0.0069 ± 0.0021	0.23 ± 0.063
11	Olmesartan medoxomil	0.40 ± 0.047	0.24 ± 0.035	0.047 ± 0.020	0.20 ± 0.037

Each value presents the mean ± S.D. (n=3)

^a CL_{int} values could not be obtained. The remaining ratio of the compounds incubated for 60 min was >90%

(CL_{int} < 0.002 mL/min/mg S9 protein).

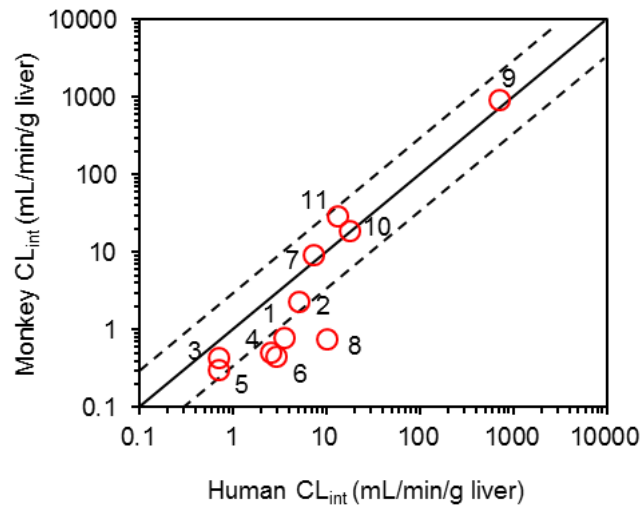
Table 5. CL_{int} values in kidney S9 of human, monkey, dog and rat

No.	Compounds	CL _{int,KS9} (mL/min/mg S9 protein)			
		human	monkey	dog	rat
9	Candesartan cilexetil	0.61 ± 0.094	2.3 ± 0.027	7.1 ± 0.42	1.8 ± 1.2
10	Mycophenolate mofetil	0.12 ± 0.012	5.3 ± 0.51	5.6 ± 0.85	1.0 ± 0.14
11	Olmesartan medoxomil	0.21 ± 0.048	0.86 ± 0.067	0.13 ± 0.048	0.38 ± 0.030

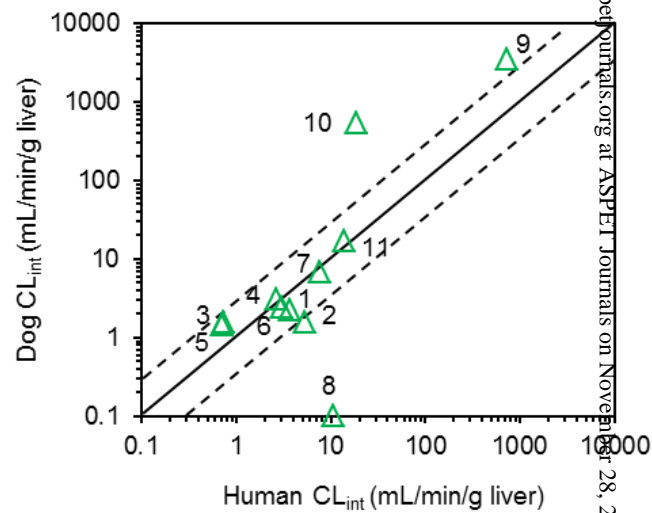
Each value presents the mean ± S.D. (n=3)

Figure 1

(A) Monkey



(B) Dog



(C) Rat

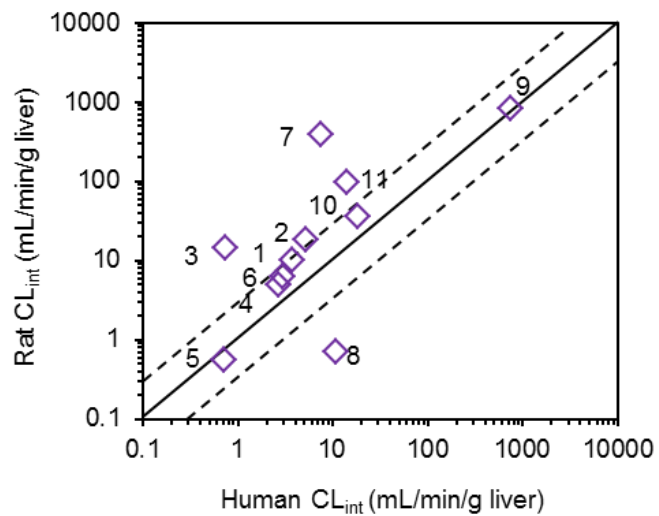
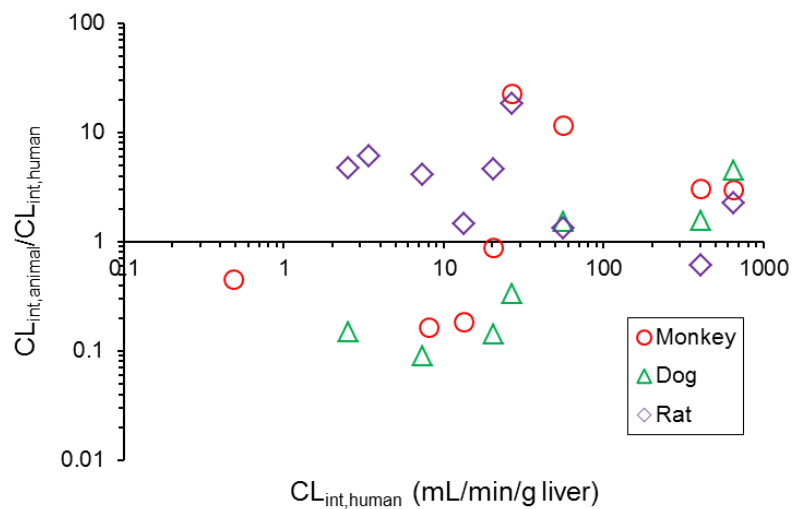
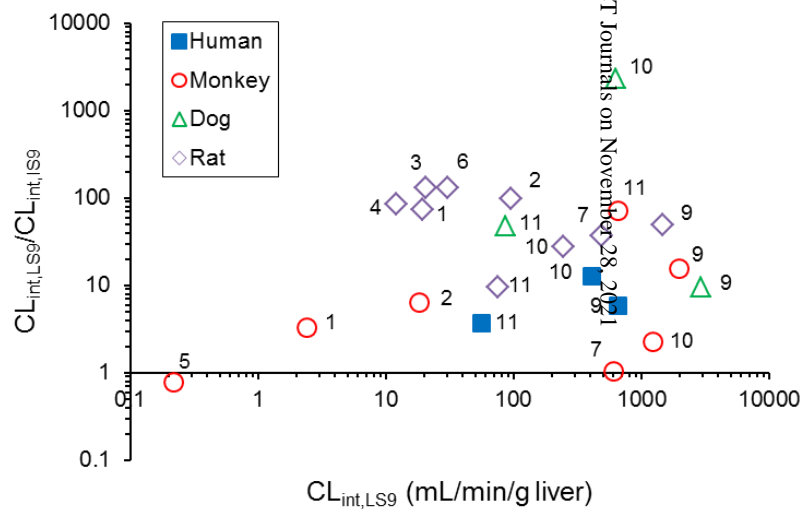


Figure 2

(A) Liver S9



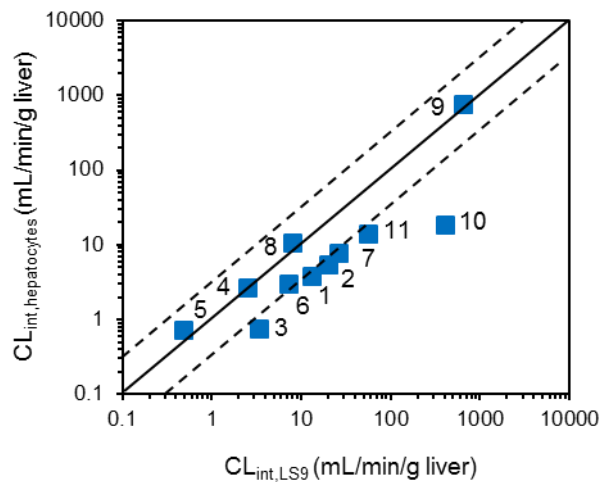
(B) Intestinal vs. Liver S9



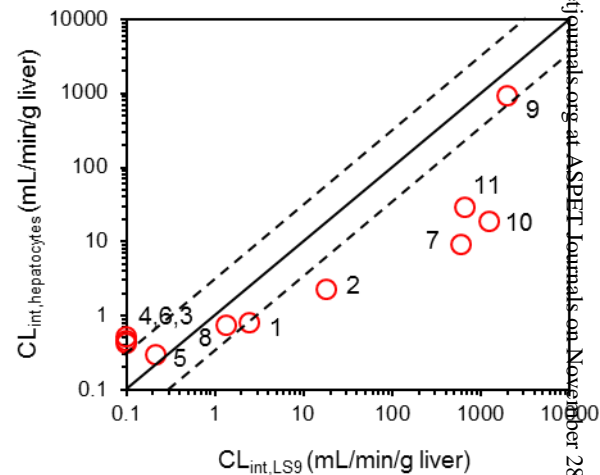
Downloaded from dmd.aspetjournals.org at ASPET Journals on November 28, 2015

Figure 3

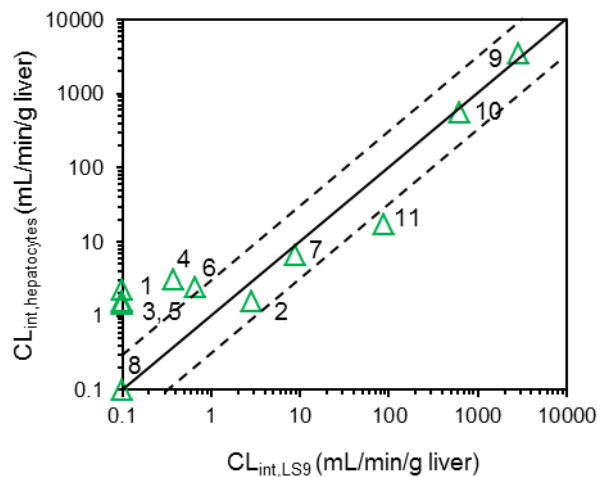
(A) Human



(B) Monkey



(C) Dog



(D) Rat

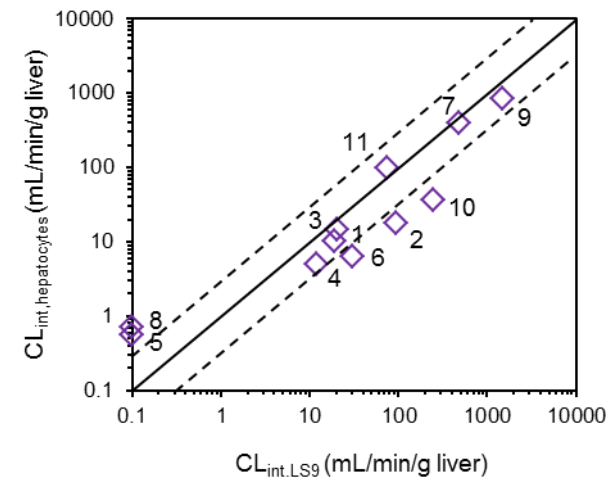


Figure 4

